

Thermocapillary motion on lubricant-impregnated surfaces

Nada Bjelobrk,¹ Henri-Louis Girard,¹ Srinivas Bengaluru Subramanyam,² Hyuk-Min Kwon,¹
David Quéré,^{3,*} and Kripa K. Varanasi^{1,*}

¹*Department of Mechanical Engineering, Massachusetts Institute of Technology, 77 Massachusetts Avenue,
Cambridge, Massachusetts 02139-4307, USA*

²*Department of Materials Science and Engineering, Massachusetts Institute of Technology,
77 Massachusetts Avenue, Cambridge, Massachusetts 02139-4307, USA*

³*Laboratoire de Physique et Mécanique des Milieux Hétérogènes, UMR No. 7636 du CNRS,
ESPCI, 75005 Paris, France*

(Received 28 March 2016; published 14 October 2016)

We show that thermocapillary-induced droplet motion is markedly enhanced when using lubricant-impregnated surfaces as compared to solid substrates. These surfaces provide weak pinning, which makes them ideal for droplet transportation and specifically for water transportation. Using a lubricant with viscosity comparable to that of water and temperature gradients as low as 2 K/mm, we observe that drops can propel at 6.5 mm/s, that is, at least 5 times quicker than reported on conventional substrates. Also in contrast with solids, the liquid nature of the different interfaces makes it possible to predict quantitatively the thermocapillary Marangoni force (and velocity) responsible for the propulsion.

DOI: [10.1103/PhysRevFluids.1.063902](https://doi.org/10.1103/PhysRevFluids.1.063902)

Droplet mobility on solid surfaces is crucial for many applications including repellency [1,2], self-cleaning [3], anti-icing [4], microfluidics [5], dropwise condensation [6,7], and fog collection [8]. The mobility of drops can be lowered or even impeded by substrate heterogeneities that result in contact line pinning [9–13]. Hence it is worth thinking of devices that simultaneously provide propulsion and reduce pinning. Droplets tend to move towards more wettable regions [14], and substrates with spatial gradients in surface energy [14–17], substrate stiffness [18], and/or temperature have been used to drive liquids [19–25].

Thermocapillary effects have also been exploited to move, merge, and split drops through rapidly changing heating patterns [25], with applications in biology and chemistry [26,27]. A thermal gradient alters the surface tension of the liquid and induces a shear flow, which can contribute to the propulsion of droplets [19]. Very commonly, imperfections of the substrate necessitate the application of large temperature gradients on the order of several K/mm [21–24], rendering the technique energy intensive and incompatible with many applications. For a given thermal gradient, the temperature difference between the two ends of a drop and the corresponding driving force can be enhanced by increasing the contact area between the liquid and the substrate [20], but this also increases viscous resistance. As a result, the above-mentioned approaches constrain the choice and size of the test liquids. In particular, transporting water droplets using thermocapillarity has been challenging because of large contact angles or contact angle hysteresis. Hence there is a need for slippery surfaces that can achieve thermocapillary motion at much lower temperature gradients. Here we propose a solution consisting of a lubricant-impregnated substrate subjected to a temperature gradient.

Lubricant-impregnated surfaces (LISs) are textured materials imbibed by a lubricant [9,28–33]. A drop on a LIS can exist in one of twelve different thermodynamic states depending on the properties of the droplet, impregnating liquid, solid texture, and surrounding environment [30]. Stable impregnation requires the contact angle of the impregnating liquid to be less than a critical angle θ_c , given by the expression $\theta_c = \cos^{-1} (1 - \varphi)/(r - \varphi)$, where φ is the fraction of the projected area of

*Corresponding authors: david.quere@espci.fr; varanasi@mit.edu

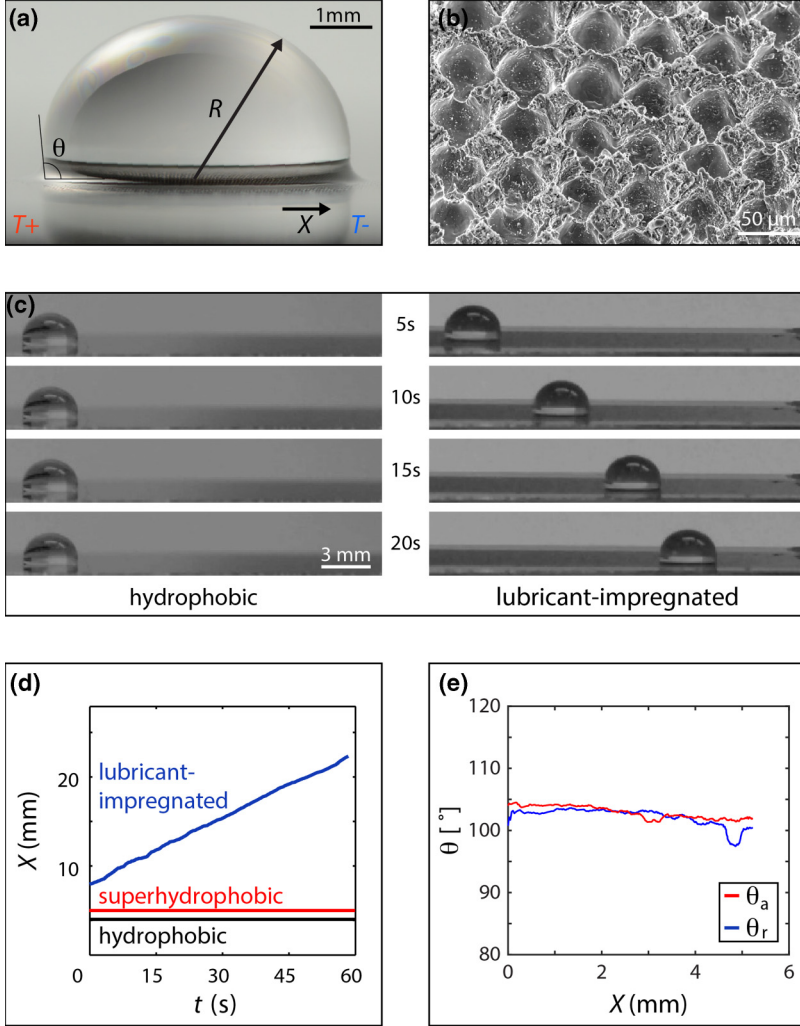


FIG. 1. (a) Water drop on a lubricant-impregnated surface subjected to a thermal gradient. The substrate is shining, owing to the presence of silicone oil imbibing its texture; oil also produces a ridge around the drop and iridescence around the cap. (b) SEM picture of the laser-textured silicon substrate showing a hierarchical surface with $80\text{-}\mu\text{m}$ -high posts covered with nanostructures. (c) Chronophotography of water drops with volume $\Omega = 10\text{ }\mu\text{L}$ exposed to a temperature gradient $dT/dx = -1.8\text{ K/mm}$ on smooth hydrophobic surface and on a LIS (with oil viscosity $\mu_o = 7.5\text{ mPa s}$ at 40°C). (d) Corresponding droplet position X obtained from the videos as a function of time t on a LIS (for $\mu_o = 40\text{ mPa s}$) and on hydrophobic and superhydrophobic materials. (e) Apparent contact angle θ on a LIS as a function of position X , as water self-propels under a thermal gradient. Advancing and receding angles are found to nearly superimpose.

the surface that is occupied by the solid and r is the roughness of the substrate. The submergence or exposure of texture tops under the droplet is dictated by the spreading coefficient of the impregnating liquid (o) on the solid (s) in the presence of the droplet (w), given by $S_{os(w)} = \gamma_{sw} - \gamma_{os} - \gamma_{ow}$, where γ is the interfacial energy. In the case of complete spreading of the lubricant on the surface ($S_{os(w)} > 0$), a thin van der Waals film submerges the tops of textures and weakens or even eliminates pinning sites [30]. A drop in such a state [Fig. 1(a)] is highly mobile.

Silicon substrates with hierarchical texture comprising $80\text{-}\mu\text{m}$ -high posts covered with nanostructures [Fig. 1(b)] were fabricated using laser ablation [34]. Hydrophobic treatment by

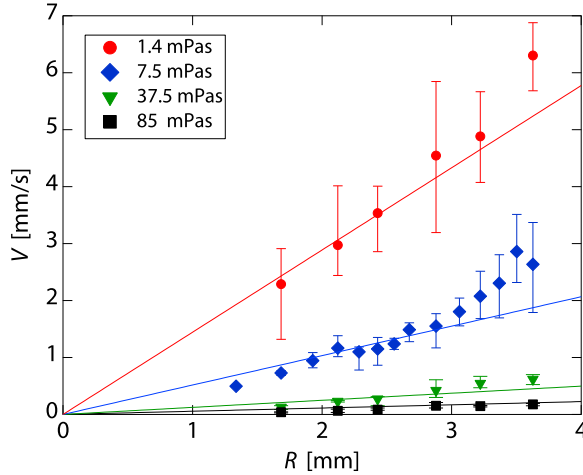


FIG. 2. Steady-state velocity V of drop thermomigration as a function of the drop radius R for lubricant (silicone oil) viscosities between 1.4 and 85 mPa·s (at 40 °C). Symbols are used for experimental values, while solid lines show linear fits corresponding to Eq. (2). Videos of droplet propulsion on lubricant-impregnated surfaces at various viscosities are available in Ref. [34].

octadecyltrichlorosilane (OTS) ensures complete wetting by the silicone oils used as lubricants. Water meets the impregnated material with identical apparent advancing and receding contact angles $\theta_a \approx \theta_r = 102^\circ \pm 5^\circ$, showing a negligible contact angle hysteresis [30]. The lubricant forms a wetting ridge around the contact line [Fig. 1(a)] to satisfy the balance of surface tensions. In addition, a thin cloaking film covers the droplet if the spreading parameter $S = \gamma_{wa} - \gamma_{oa} - \gamma_{ow}$ of lubricant on water is positive [30]. The spreading parameter S can be predicted: In our case, its value decreases from 12 mN/m to 7 mN/m as temperature increases from $T_- = 20^\circ\text{C}$ to $T_+ = 65^\circ\text{C}$. We anticipate from its positive value the existence of a cloaking film in our system, as confirmed by iridescences at the drop surface in Fig. 1(a).

When a thermal gradient ($dT/dx = -1.8$ K/mm) is applied along the x axis defined in Fig. 1(a), we observe that water droplets propel from hot to cold regions [Figs. 1(c) and 1(d)]. The apparent contact angle θ (and thus the drop shape) remains nearly constant along the motion, as visible in Fig. 1(c) and reported in Fig. 1(e). Propulsion is maintained for multiple sequential droplets, showing there is no significant depletion of silicone oil from the substrate during experiments, in agreement with [32]. In contrast, no thermocapillary propulsion of water drops is observed on smooth hydrophobic (OTS functionalized) surfaces, as shown in Figs. 1(c) and 1(d) [34]. The contact angle hysteresis ($\sim 14^\circ$) on the smooth hydrophobic surface is large enough to oppose the thermocapillary force. On superhydrophobic materials, no motion is observed either: Hysteresis is smaller (below 3°) but the large water contact angle ($153^\circ \pm 3^\circ$) results in a 60% smaller droplet base radius than that on LISs, which leads to a lower surface tension contrast and thus a weaker thermocapillary force.

As shown in Figs. 1(c) and 1(d), droplets on LISs quickly reach a uniform velocity V (of about 0.25 mm/s in the plot), which suggests a steady state where a thermocapillary driving force balances viscous resistance. We compare in Fig. 2 the velocity V obtained for droplet radii $R = 1 - 4$ mm and lubricant viscosities $\mu_o = 1 - 100$ mPa·s (given at the average temperature of 40 °C), at fixed thermal gradient. On the one hand, the velocity V increases with the radius R due to a higher surface tension difference across the droplet and thus a higher thermocapillary force [20,21]. The strong dependence on radius confirms that propulsion is based on thermocapillarity and not simply lubricant migration due to the temperature gradient [20,21,32]. On the other hand, motion is faster for smaller μ_o . By choosing a silicone oil with a viscosity $\mu_o = 1.4$ mPa·s (red circles in Fig. 2), an

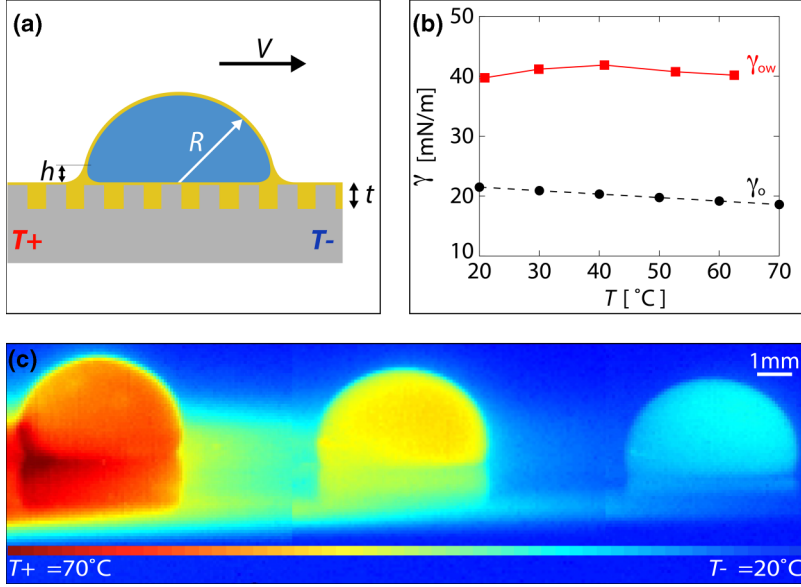


FIG. 3. (a) Sketch of a drop on a lubricant-impregnated surface exposed to a temperature gradient. (b) Variations of the oil-water and oil-air surface tensions γ_{ow} and γ_o as a function of temperature T [34]. The oil here has a viscosity $\mu_o = 7.5$ mPa s at 40 $^{\circ}\text{C}$. (c) Images from an infrared video showing the thermocapillary-induced motion of a droplet of water ($\Omega = 30$ μL) moving on a LIS impregnated with a silicone oil ($\mu_o = 7.5$ mPa s) and subjected to a temperature gradient $dT/dx = -1.8$ K/mm. See Ref. [33].

enhancement of more than one order of magnitude is achieved when compared to a silicone oil of viscosity $\mu_o = 85$ mPa s (black squares) or to solid substrates in Refs. [20–24].

As sketched in Fig. 3(a), the reason why drops move under a temperature gradient arises from the presence of multiple interfaces whose interfacial tension varies with temperature. We report in Fig. 3(b) the variations of oil-air and oil-water interfacial tensions, respectively denoted by γ_o and γ_{ow} , which were measured using a tensiometer [34]. We base our model on the following observations: (i) The drop constantly adopts the substrate temperature $T(x)$, as observed in Fig. 3(c), which shows successive infrared images along the motion, and (ii) the drop shape remains constant, as shown in Figs. 1(c), 1(e), and 3(c); for the sake of simplicity, we treat the spherical cap as a hemisphere (contact angle of 90 $^{\circ}$), so that the drop base and spherical cap have a common radius R .

Owing to temperature differences between both sides on the drop, surface tensions do not balance, which yields, as a resulting force F acting on the drop,

$$F \approx \pi R^2 [(d\gamma_o/dT) - (d\gamma_{ow}/dT)](dT/dx). \quad (1)$$

The temperature gradient dT/dx is negative, so the variation of oil surface tension with T ($d\gamma_o/dT < 0$ [Fig. 3(b)]) is found to propel the drop to the right ($F > 0$): As water moves to the cold region, it “erases” an area πR^2 of oil of higher energy. The role of oil-water surface tension is more ambiguous: At the beginning of motion (hot region), γ_{ow} is quasi-independent of T ($d\gamma_{ow}/dT \approx 0$ [Fig. 3(b)]) and it does not contribute to motion. Later, in cooler regions (below 4 $^{\circ}\text{C}$ [Fig. 3(b)]), we have $d\gamma_{ow}/dT \geq 0$ and both tensions γ_o and γ_{ow} draw water to the cold region.

Despite the motion, the drop hardly changes its shape [Figs. 1(c), 1(e), and 3(c)]. The apparent contact angle is given by Young’s formula, which can be written for a cloaked drop on the LIS [Fig. 3(a)]: $\cos \theta = (\gamma_o - \gamma_{ow})/(\gamma_o + \gamma_{ow})$, where both γ_o and γ_{ow} are measurable. For $\gamma_o \approx 20$ mN/m and $\gamma_{ow} \approx 42$ mN/m, we get $\theta = 110^{\circ}$, close to the observed value. As the drop moves, and considering that γ_{ow} hardly changes with temperature, we expect $\Delta \theta \approx -2\Delta \gamma_o \gamma_{ow}/(\gamma_o + \gamma_{ow})^2$, that is $-2^{\circ} - 3^{\circ}$, a small variation indeed, yet consistent with the data in Fig. 1(e).

The quantity we access experimentally is the drop velocity V , which results from a balance between the force driving the motion and hydrodynamic resistance. Reynolds numbers here are small, even for the smallest oil viscosity where it is on the order of 10^{-2} . Viscous friction can have different origins. (i) For oil viscosity μ_o larger than water viscosity μ_w , the respective contributions of viscous forces in the drop and in the oil film scale as $(\mu_w V/R)\pi R^2$ and $(\mu_o V_i/t)\pi R^2$, where t is the height of the texture and V_i is the slip velocity at the oil-water interface. Continuity of stress at this interface allows us to express the slip velocity. We have $V_i \sim (\mu_w/\mu_o)(t/R)V$, which is much smaller than V and logically vanishing as μ_o diverges. Hence both viscous contributions are equivalent and found to scale as $\mu_w V\pi R$, an expression independent of oil viscosity. (ii) A specific feature of LISs is the existence of a liquid ridge (of typical size h) at the contact line, as can be observed in Fig. 1(a) and sketched in Fig. 3(a). This ridge moves with the drop, and it was proposed in [30] to be the main source of dissipation for liquids running down inclined LISs. The corresponding viscous force should scale as $(\mu_o V/h)\pi R h \sim \mu_o V\pi R$, an expression independent of the unknown distance h and proportional to both drop size R and oil viscosity μ_o . Hence the total viscous resistance can be expressed as $\alpha(\mu_o + 2\mu_w)V\pi R$, where α is a numerical factor. Balancing this viscous force with the thermocapillary force expressed in Eq. (1), we find an expression for the drop velocity V :

$$V \approx (1/\alpha)R(d\hat{\gamma}/dT)(dT/dx)/(\mu_o + 2\mu_w), \quad (2)$$

where we denote by $\hat{\gamma} = \gamma_o - \gamma_{ow}$ the effective tension driving the motion. Equation (2) qualitatively agrees with our observations in Fig. 2: The velocity V increases with the drop size and the variation is indeed close to being linear; in addition, motion is slower on more viscous substrates, for a fixed size R . A quantitative agreement seems difficult to establish at first glance: As deduced from Fig. 3(b), the driving force can increase as motion proceeds, but oil simultaneously becomes more viscous in the cooler regions. On the one hand, the quantity $d\gamma_o/dT$ is about $-0.06 \text{ mN m}^{-1}\text{K}^{-1}$ and $-d\gamma_{ow}/dT$ in the cool region can be on the same order [Fig. 3(b)], so the driving force typically doubles in this region; on the other hand, viscosity of silicone oil increases by a factor 2 between 65°C and 20°C . Hence drop velocity can remain roughly constant [as shown in Fig. 1(d)], the increase of driving force being compensated for by the increase of viscous resistance.

In order to compare our data to Eq. (2), we consider a mean gradient of surface tension $d\hat{\gamma}/dT \approx -0.06 \text{ mN m}^{-1}\text{K}^{-1}$ and a mean viscosity $\mu = \mu_o$, both determined at the average temperature of the substrate (around 40°C). For cases where the viscosity of oil compares to that of water, we add to the oil viscosity twice the water viscosity, corresponding to dissipation in the drop and in the film, as discussed earlier. We draw in Fig. 2 the corresponding line and find satisfactory agreement with all the data provided we choose $\alpha \approx 22$ (same value for all fits). This numerical coefficient is close to the one determined for water drops running down inclined liquid-impregnated materials, for which the driving force is the known weight of drops, and the coefficient in the viscous force is similarly treated as an adjustable parameter and found to be ~ 27 [30].

It was found that propulsion is triggered by differences of surface tension [Eq. (1)], which implies that the direction of motion (hot to cold here) might be reversed by choosing an appropriate lubricant-droplet pair. Since the tension of oil decreases with temperature, obtaining the reverse motion (from cold to hot) would require $d\gamma_{ow}/dT$ to be larger in absolute value than $d\gamma_o/dT$. In the same vein, motion can be stopped for pairs of liquids with $d\gamma_{ow}/dT \approx d\gamma_o/dT$, which is the case if tetradecane is used as a lubricant, as variations of both the interfacial tensions are $-0.09 \text{ mN m}^{-1}\text{K}^{-1}$. Indeed, we found that water does not propel anymore when placed on a tetradecane-impregnated solid with a similar temperature gradient. These remarks emphasize that thermocapillary motion on LISs allows one to have an explicit, predictable form for the driving force, which involves measurable quantities only, unlike on solids. It also provides a control of the drop velocity along the motion, since both the driving force and the lubricant viscosity can be temperature dependent. This system thus appears highly tunable, exploiting the unique characteristics of liquid-impregnated surfaces.

In summary, we showed that lubricant-impregnated surfaces promote thermocapillary motion of liquids for several reasons. Pinning is strongly reduced on LISs, rendering droplets very mobile. On a regular solid substrate, thermocapillary forces must overcome pinning, and even above the corresponding threshold in temperature gradient, angle hysteresis opposes the motion, whose speed remains quite modest. An at least fivefold increase in velocity can be achieved on LISs compared to solid substrates for the same temperature gradient and droplet volume [21,22]. Specifically, propulsion of water at appreciable velocities is made possible. In addition, the apparent contact angle on LISs is typically around 90° , that is, low enough to provide significant contact with the substrate and thus significant temperature differences between both edges of the deposited droplet, unlike what is observed on superhydrophobic surfaces for which contact is minimized.

We thank J. Buongiorno, T. McKrell, and C. J. Love for IR videos; R. Cohen, G. McKinley, and J. Kleingartner for help with IFT measurements; F. Frankel for help with photographs; and J. D. Smith for the data on isothermal gravity experiments. The authors acknowledge MIT-France program and the Swiss National Science Foundation (Grant No. PBEZP2_145959).

N.B. and H.-L.G. contributed equally to this work.

-
- [1] T. M. Schutzius, S. Jung, T. Maitra, G. Graeber, M. Köhme, and D. Poulikakos, Spontaneous droplet trampolining on rigid superhydrophobic surfaces, *Nature (London)* **527**, 82 (2015).
 - [2] L. Bocquet and E. Lauga, A smooth future? *Nat. Mater.* **10**, 334 (2011).
 - [3] X. Deng, L. Mammen, H.-J. Butt, and D. Vollmer, Candle soot as a template for a transparent robust superamphiphobic coating, *Science* **335**, 67 (2012).
 - [4] A. J. Meuler, G. H. McKinley, and R. E. Cohen, Exploiting topographical texture to impart icephobicity, *ACS Nano* **4**, 7048 (2010).
 - [5] A. M. Pit, R. De Ruiter, A. Kumar, D. Wijnperlé, M. H. G. Duits, and F. Mugele, High-throughput sorting of drops in microfluidic chips using electric capacitance, *Biomicrofluidics* **9**, 044116 (2015).
 - [6] N. A. Patankar, Supernucleating surfaces for nucleate boiling and dropwise condensation heat transfer, *Soft Matter* **6**, 1613 (2010).
 - [7] V. P. Carey, *Liquid-Vapor Phase-Change Phenomena: An Introduction to the Thermophysics of Vaporization and Condensation Processes in Heat Transfer Equipment*, 2nd ed. (Taylor and Francis, New York, 2008).
 - [8] J. Ju, H. Bai, Y. Zheng, T. Zhao, R. Fang, and L. Jiang, A multi-structural and multi-functional integrated fog collection system in cactus, *Nat. Commun.* **3**, 1247 (2012).
 - [9] D. Quéré, Non-sticking drops, *Rep. Prog. Phys.* **68**, 2495 (2005).
 - [10] X. Chen, R. Ma, J. Li, C. Hao, W. Guo, B. L. Luk, S. C. Li, S. Yao, and Z. Wang, Evaporation of Droplets on Superhydrophobic Surfaces: Surface Roughness and Small Droplet Size Effects, *Phys. Rev. Lett.* **109**, 116101 (2012).
 - [11] U. Thiele and E. Knobloch, Driven Drops on Heterogeneous Substrates: Onset of Sliding Motion, *Phys. Rev. Lett.* **97**, 204501 (2006).
 - [12] W. Xu and C. Choi, From Sticky to Slippery Droplets: Dynamics of Contact Line Depinning on Superhydrophobic Surfaces, *Phys. Rev. Lett.* **109**, 024504 (2012).
 - [13] S. Varagnolo, D. Ferraro, P. Fantinel, M. Pierno, G. Mistura, G. Amati, L. Biferale, and M. Sbragaglia, Stick-Slip Sliding of Water Drops on Chemically Heterogeneous Surfaces, *Phys. Rev. Lett.* **111**, 066101 (2013).
 - [14] M. K. Chaudhury and G. M. Whitesides, How to make water run uphill, *Science* **256**, 1539 (1992).
 - [15] S. Daniel, M. K. Chaudhury, and J. C. Chen, Fast drop movements resulting from the phase change on a gradient surface, *Science* **291**, 633 (2001).
 - [16] G. Fang, W. Li, X. Wang, and G. Qiao, Droplet motion on designed microtextured superhydrophobic surfaces with tunable wettability, *Langmuir* **24**, 11651 (2008).

- [17] C. Sun, X.-W. Zhao, Y.-H. Han, and Z.-Z. Gu, Control of water droplet motion by alteration of roughness gradient on silicon wafer by laser surface treatment, *Thin Solid Films* **516**, 4059 (2008).
- [18] R. W. Style, Y. Che, S. J. Park, B. M. Weon, J. H. Je, C. Hyland, G. K. German, M. P. Power, L. A. Wilen, J. S. Wettlaufer, and E. R. Dufresne, Patterning droplets with durotaxis, *Proc. Natl. Acad. Sci. USA* **110**, 12541 (2013).
- [19] F. Brochard, Motions of droplets on solid surfaces induced by chemical or thermal gradients, *Langmuir* **5**, 432 (1989).
- [20] J. B. Brzoska, F. Brochard-Wyart, and F. Rondelez, Motions of droplets on hydrophobic model surfaces induced by thermal gradients, *Langmuir* **9**, 2220 (1993).
- [21] J. Z. Chen, S. M. Troian, A. A. Darhuber, and S. Wagner, Effect of contact angle hysteresis on thermocapillary droplet actuation, *J. Appl. Phys.* **97**, 014906 (2005).
- [22] V. Pratap, N. Moumen, and R. S. Subramanian, Thermocapillary motion of a liquid drop on a horizontal solid surface, *Langmuir* **24**, 5185 (2008).
- [23] A. Gao, X. Liu, T. Li, X. Gao, and Y. Wang, Thermocapillary actuation of droplets on a microfluidic chip, *J. Adhesion Sci. Technol.* **26**, 2165 (2012).
- [24] Y. Zhao, F. Liu, and C.-H. Chen, Thermocapillary actuation of binary drops on solid surfaces, *Appl. Phys. Lett.* **99**, 104101 (2011).
- [25] M.-C. Liu, J.-G. Wu, M.-F. Tsai, W.-S. Yu, P.-C. Lin, I.-C. Chiu, H.-A. Chin, I.-C. Cheng, Y.-C. Tung, and J.-Z. Chen, Two dimensional thermoelectric platforms for thermocapillary droplet actuation, *RSC Adv.* **2**, 1639 (2012).
- [26] A. A. Darhuber, J. P. Valentino, S. M. Troian, and S. Wagner, Thermocapillary actuation of droplets on chemically patterned surfaces by programmable microheater arrays, *J. Microelectromech. Syst.* **12**, 873 (2003); A. A. Darhuber, J. P. Valentino, J. M. Davis, S. M. Troian, and S. Wagner, Microfluidic actuation by modulation of surface stresses, *Appl. Phys. Lett.* **82**, 657 (2003).
- [27] A. A. Darhuber, J. P. Valentino, and S. M. Troian, Planar digital nanoliter dispensing system based on thermocapillary actuation, *Lab Chip* **10**, 1061 (2010).
- [28] A. Lafuma and D. Quéré, Slippery pre-suffused surfaces, *Europhys. Lett.* **96**, 56001 (2011).
- [29] T.-S. Wong, S. H. Kang, S. K. Y. Tang, E. J. Smythe, B. D. Hatton, A. Grinthal, and J. Aizenberg, Bioinspired self-repairing slippery surfaces with pressure-stable omniphobicity, *Nature (London)* **477**, 443 (2011).
- [30] J. D. Smith, R. Dhiman, S. Anand, E. Reza-Garduno, R. E. Cohen, G. H. McKinley, and K. K. Varanasi, Droplet mobility on lubricant-impregnated surfaces, *Soft Matter* **9**, 1772 (2013).
- [31] A. Carlson, P. Kim, G. Amberg, and H. A. Stone, Short and long time drop dynamics on lubricated substrates, *Europhys. Lett.* **104**, 34008 (2013).
- [32] A. Eifert, D. Paulssen, S. N. Varanakkottu, T. Baier, and S. Hardt, Simple fabrication of robust water-repellent surfaces with low contact-angle hysteresis based on impregnation, *Adv. Mater. Interfaces* **1**, 1300138 (2014).
- [33] F. Schellenberger, J. Xie, N. Encinas, A. Hardy, M. Klapper, P. Papadopoulos, H.-J. Butt, and D. Vollmer, Direct observation of drops on slippery lubricant-infused surfaces, *Soft Matter* **11**, 7617 (2015).
- [34] See Supplemental Material at <http://link.aps.org/supplemental/10.1103/PhysRevFluids.1.063902> for videos of droplet propulsion on lubricant-impregnated surfaces at various viscosities.